SELF-POWERED WIRELESS SENSORS

Fred Dynys and Ali Sayir , NASA Glenn Research Center, USA

NASA's integrated vehicle health management (IVHM) program offers the potential to improve aeronautical safety, reduce cost and improve performance by utilizing networks of wireless sensors. Development of sensor systems for engine hot sections will provide real-time data for prognostics and health management of turbo-engines. Sustainable power to embedded wireless sensors is a key challenge for prolong operation. Harvesting energy from the environment has emerged as a viable technique for power generation.

Thermoelectric generators provide a direct conversion of heat energy to electrical energy. Micro-power sources derived from thermoelectric films are desired for applications in harsh thermal environments. Silicon based alloys are being explored for applications in high temperature environments containing oxygen. Chromium based p-type Si/Ge alloys exhibit Seebeck coefficients on the order of 160 μV/K and low thermal conductance of 2.5 to 5 W/mK. Thermoelectric properties of bulk and thin film silicides will be discussed.

Self-Powered Wireless Sensors

Fred Dynys & Ali Sayir
NASA Glenn Reseach Center
Cleveland, OH

Integrated Vehicle Health Monitoring

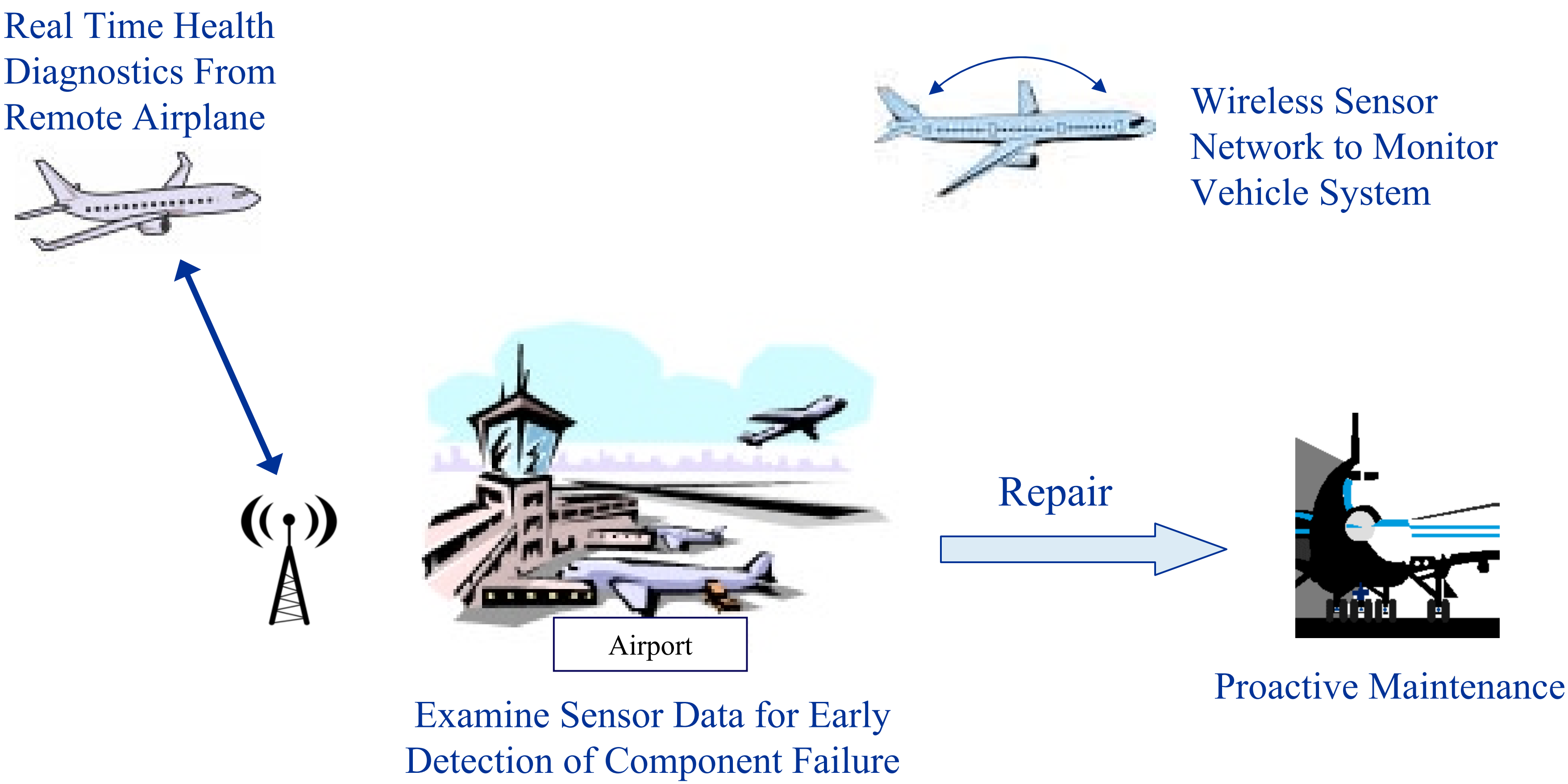

Future airplanes will have a wireless sensor network for monitoring vehicle system health, flight environment and structural integrity.

RF Wireless Sensor

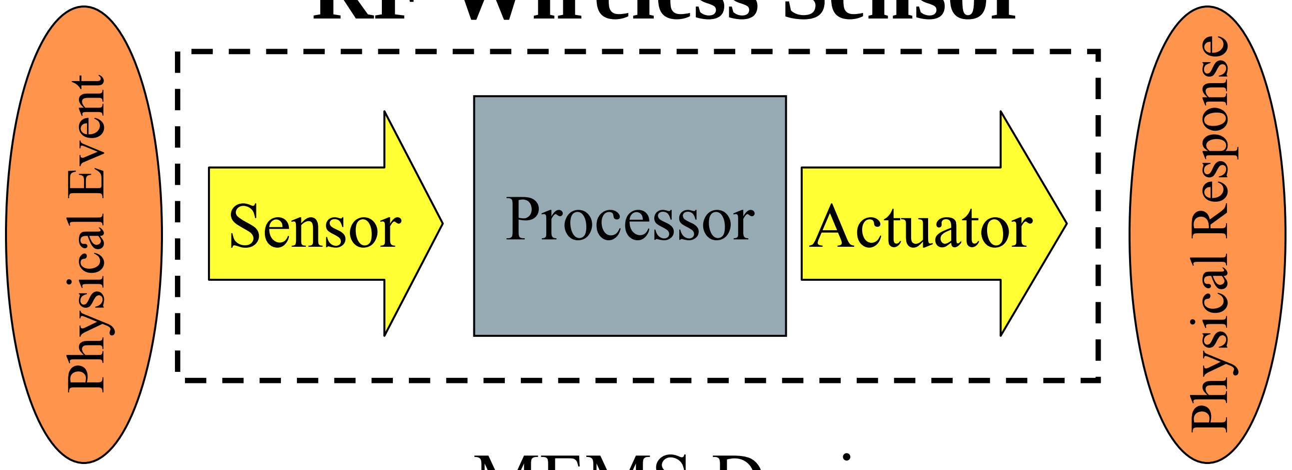

MEMS Device

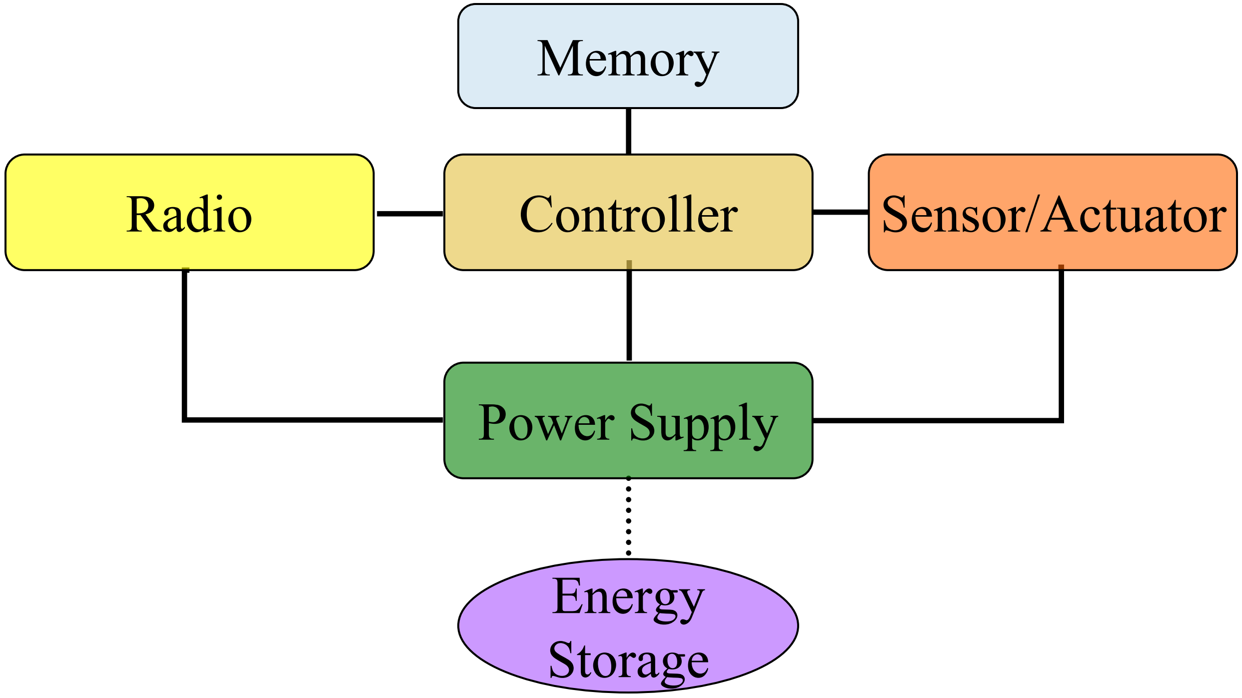

MEMS Power

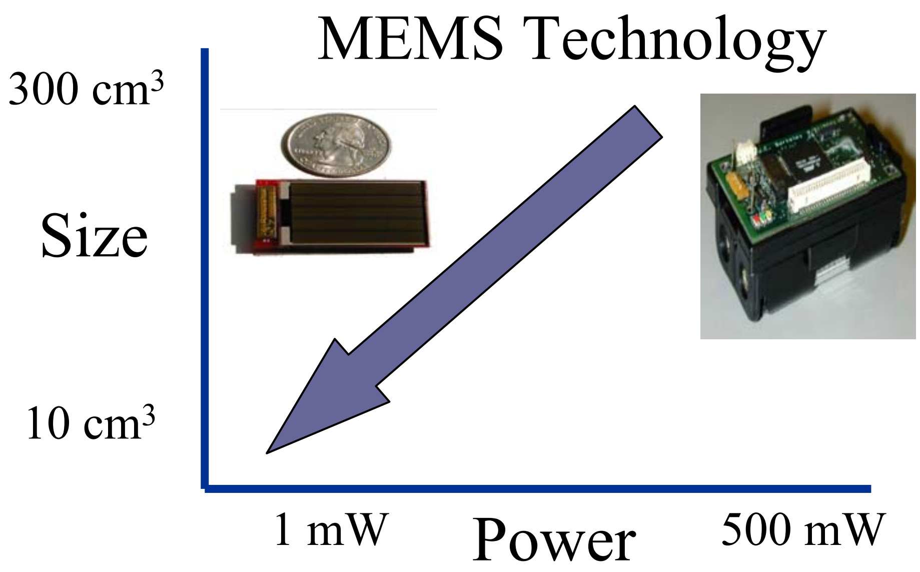

Energy Harvesting

- Reduction in MEMS energy consumption is the key to enabling energy harvesting
- Looking for renewable energy sources in the application environment.
- Infinite power source.

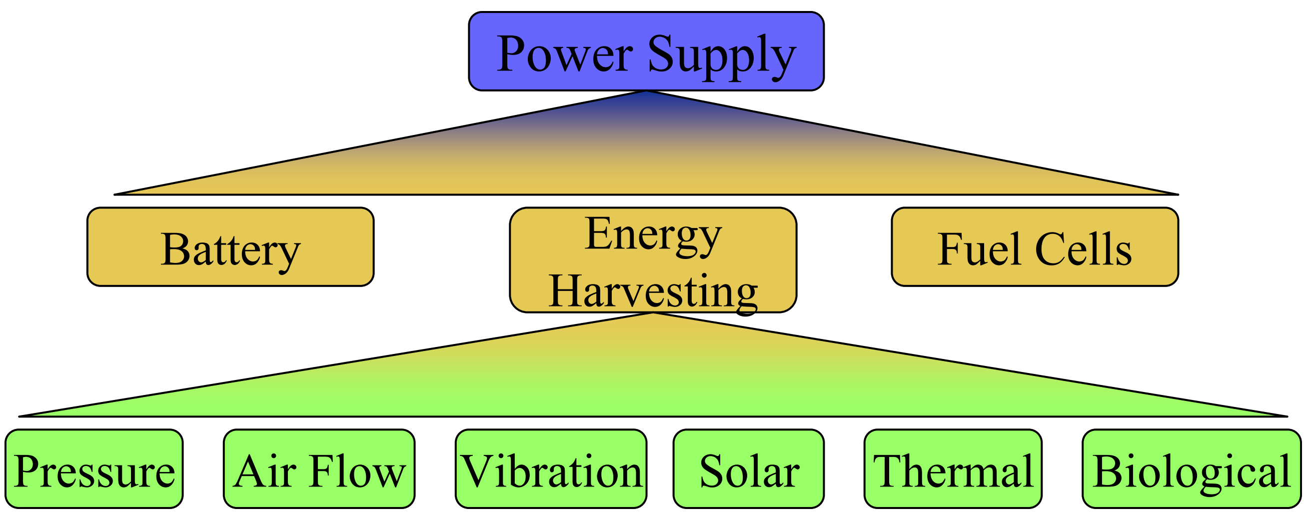

	μW/cm^3
Solar	15 -15000
Air Flow	~380
Biological	~330
Vibration	100 - 400
Thermal	<100
Pressure	<100

Wireless Sensors

Wireless technology allows sensors to be placed in remote locations

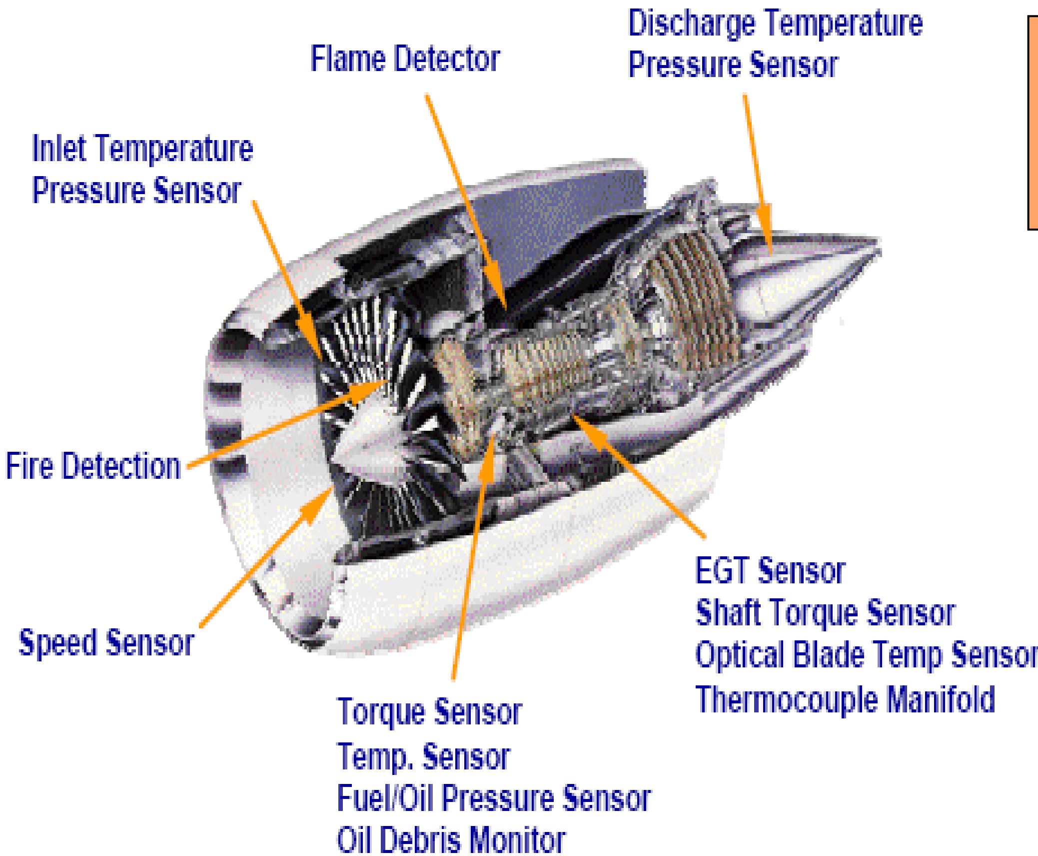

Sensors/power supply fabricated from materials that are operational in high temperature environments

GRC Sensors

Temperature

Heat Flux

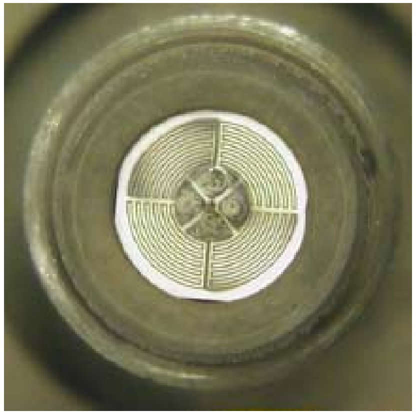

J. Wrbanek & G. Fralick

Self powered wireless sensors require technological advancement in energy harvesting

Thermoelectric Converters

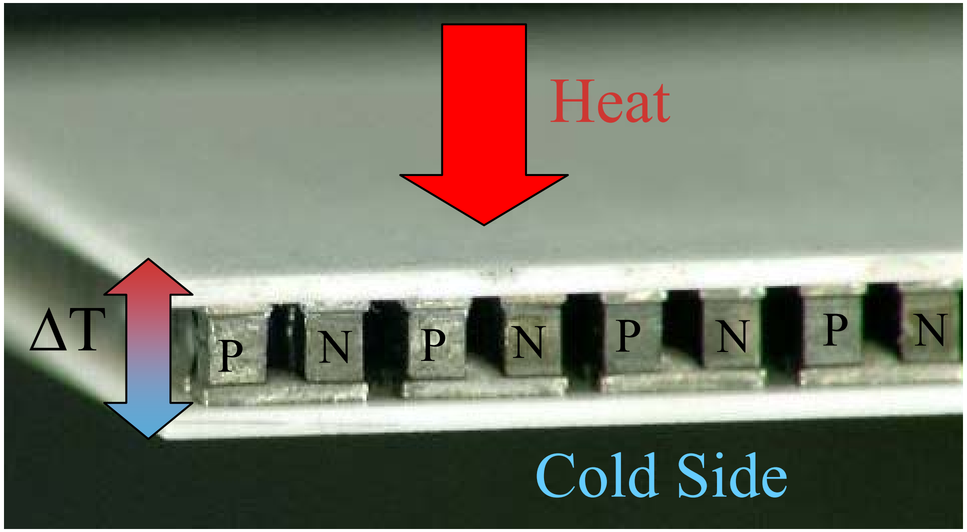

Seebeck Effect

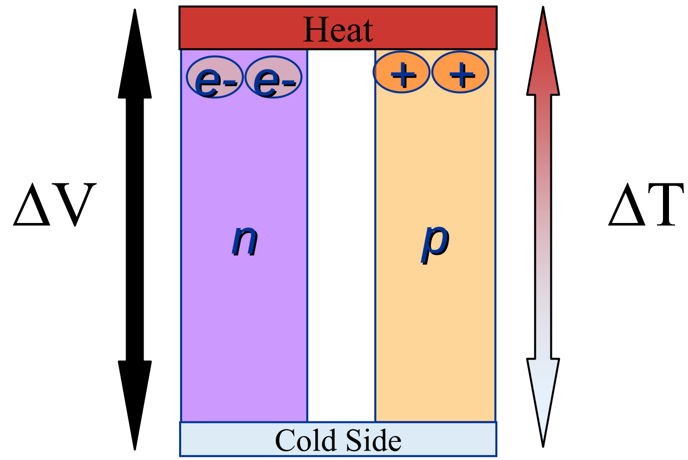

Low Efficiency (<7%) – Niche Markets

Radioisotope Thermoelectric Generator

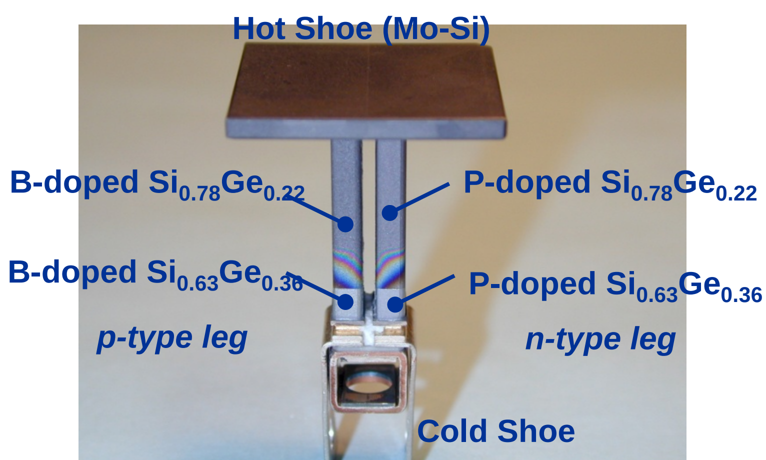

Proven Technology

- Long Life-Continuous Power- 20+ years
- Durable in Harsh Environments
- No Moving Parts

Thermoelectrics

Figure of Merit

$$ZT = \frac{S^2 \sigma}{\kappa} T$$

Desired Properties of TE's

- High Seebeck coefficient (S)
- High electrical conductivity (σ)
- Low thermal conductivity (κ)

Efficiency

$$\eta_{max} = \frac{\Delta T}{T_{hot}} \frac{\sqrt{1+ZT}-1}{\sqrt{1+ZT}+T_{cold}/T_{hot}}$$

Nanotechnology

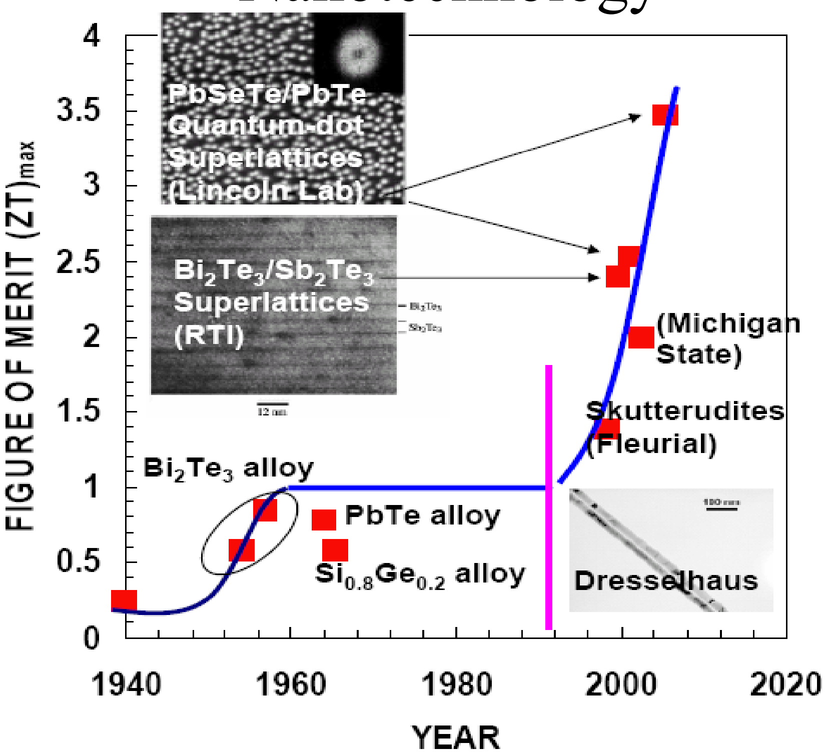

Low ΔT -Low Efficiency

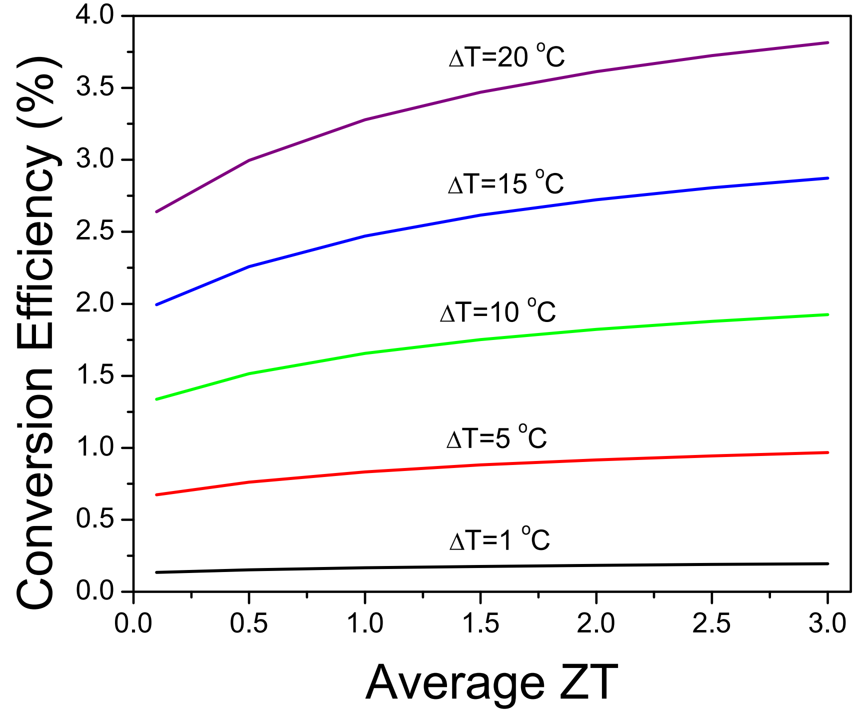

Standard Thermoelectric Materials

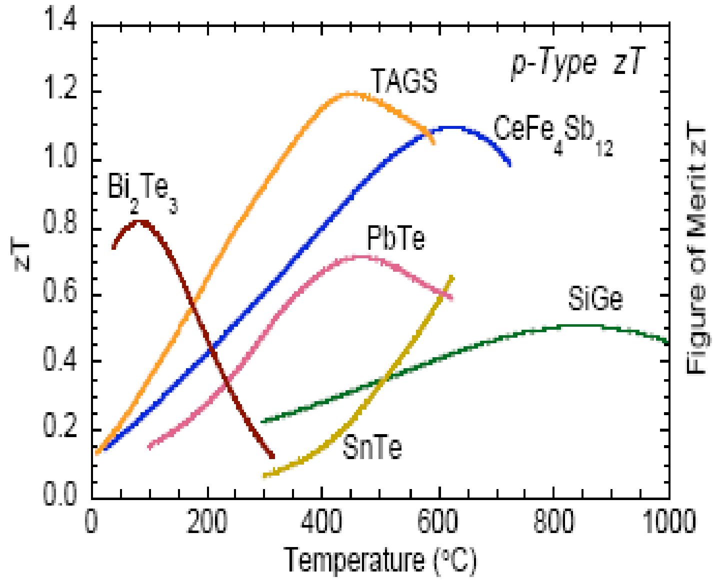

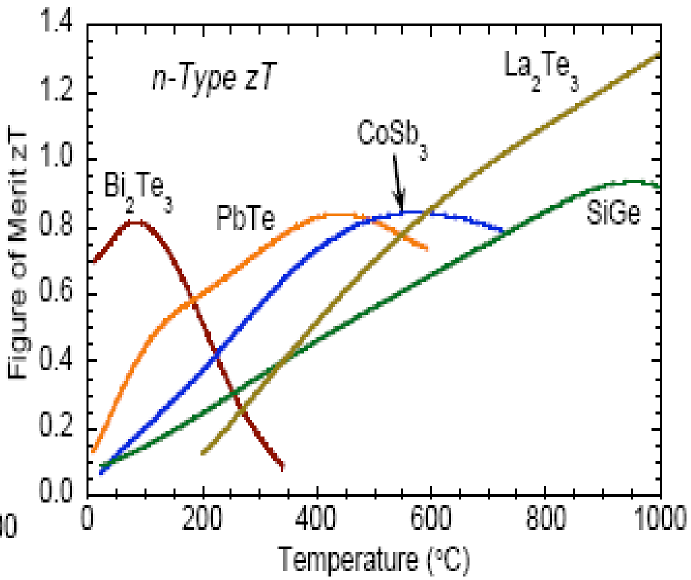

Operational Conditions

- Temperatures 300 - 600 °C
- Environment – Varying P_{O_2}

Silicides

- Environmental/Chemical Stabiltiy
- Low Electrical Resistance
- Low Formation Temperature

Electrical Transport

Semiconductor/Metallic Behavior

IIIA	IVA	VA	VIA	VIIA	VIIIA			IB
	$TiSi_2$	V_3Si V_3Si_2 V_5Si_3 VSi_2	Cr_3Si Cr_5Si_3 $CrSi_2$	$MnSi_{1.7}$	α–$FeSi_2$ β–$FeSi_2$	Co_2Si CoSi $CoSi_2$	Ni_2Si NiSi $NiSi_2$	Cu_3Si
YSi_2	$ZrSi_2$	Nb_3Si $NbSi_2$			Ru_2Si_3	$RhSi_2$	Pd_2Si	
	$HfSi_2$	$TaSi_2$		$ReSi_{1.7}$	$OsSi_2$	IrSi $IrSi_3$	PtSi	

	Band Gap	Type	Mobility Cm^2/SV	K W/mK @300 K	S mV/K @500K	ρ 10^{-5} Ω–m @500K	TE $10^{-6}/^oC$
$CrSi_2$	~0.35 ev	P	15	6.8	220	7.2	11-14
$MnSi_{1.7}$	~0.7 ev	P	40	2.9	160	3.1	16
CoSi	------	N	----	14.3	-50	0.2	11.1

Thermoelectric Module I

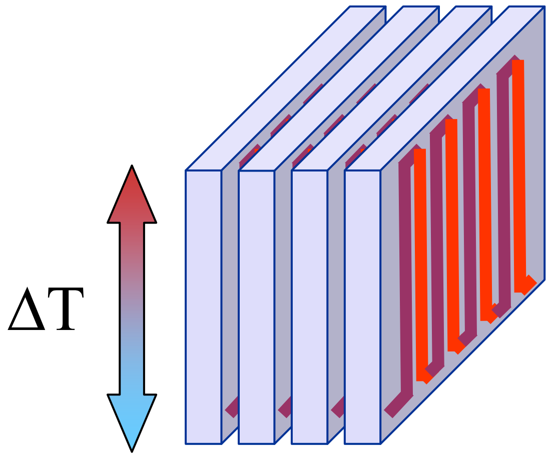

Compact geometry permits parallel connection of modules for reduced series resistance.

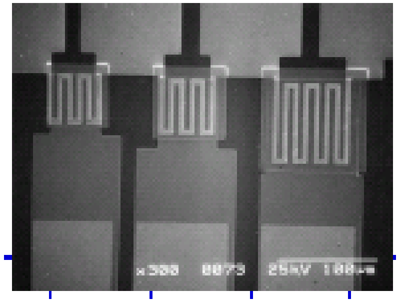

Micro-Cooler

TE Materials

- Thickness ~ 10's μm
- Electrical conductivity $\geq 10^4\ \Omega^{-1}m^{-1}$
- Larger ΔT
- Thick film stresses

Substrate

- Thickness
- Low thermal conductivity
- Electrically insulating

Interconnect Technology

- Low contact resistance

Source: P.M. Martin et al., PNNL

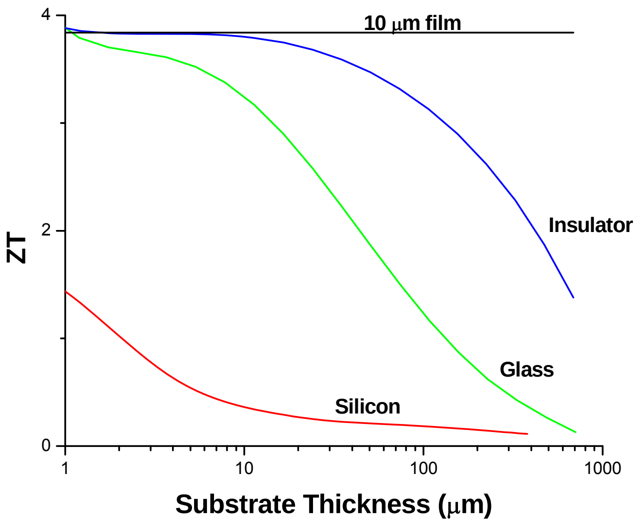

JPL

Thermoelectric Module II

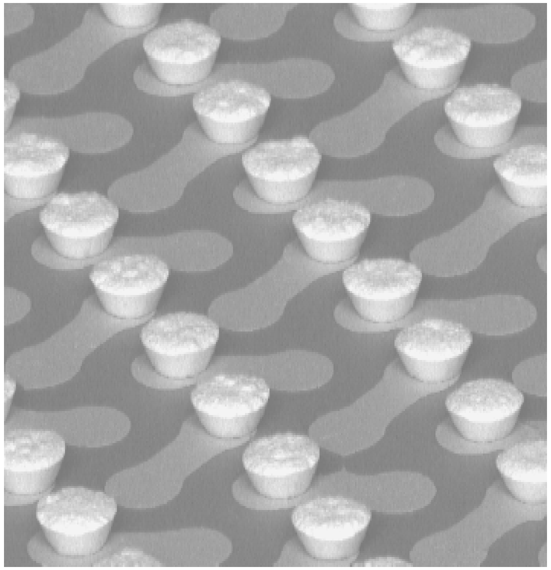

TE Materials

- Thickness ~ 100's µm
- Small ΔT – Limited TE Thickness
- Electrical Conductivity

Substrate

- Good thermal conductivity
- Electrically insulating

Interconnect Technology

- Low contact resistance

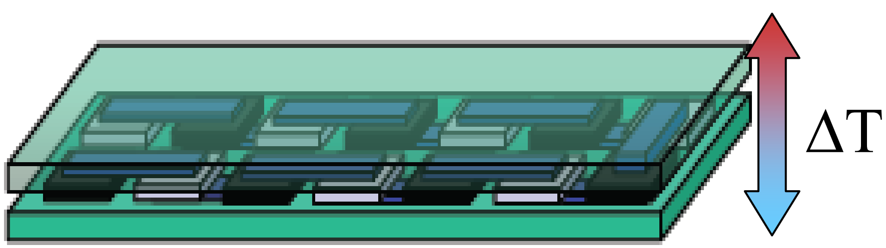

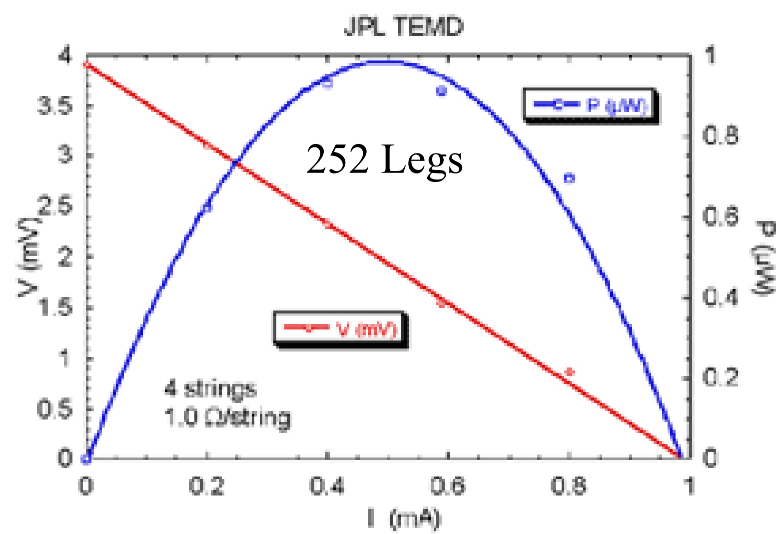

Magnetron Sputtering

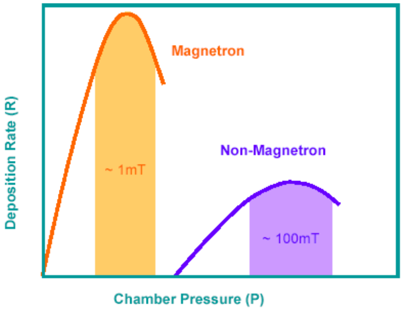

- •Lower Deposition Pressure
- •Reduces Contamination
- •Increases Deposition Rate
- •Complex Alloys

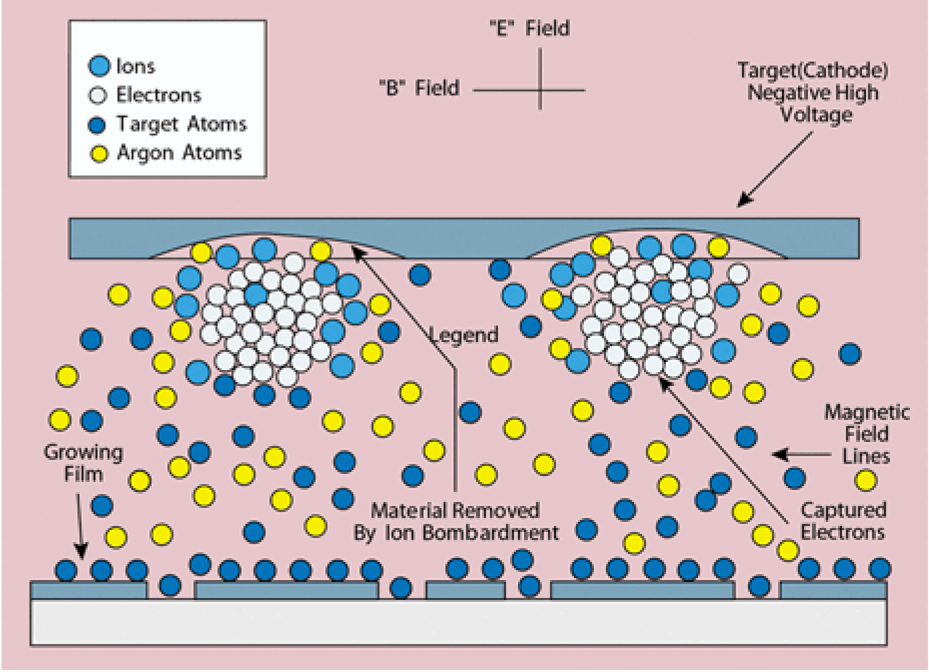

3 RF Guns 600 W

Sample Rotation

Heater RT – 800 °C

Magnetron Sputtering

Deposition Rate
- Distance – 1/(d)½
- Material
- Pressure

Targets
- Commercial Sources
- Single Crystal – B-Si, Sb-Si

Co-Sputtering
Adjust Deposition Rate To Control Composition

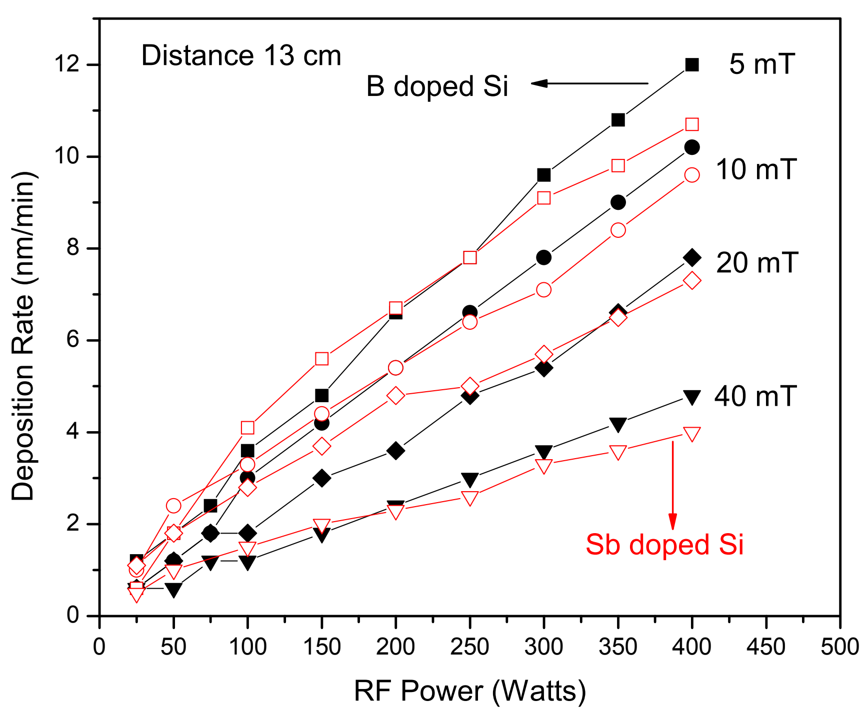

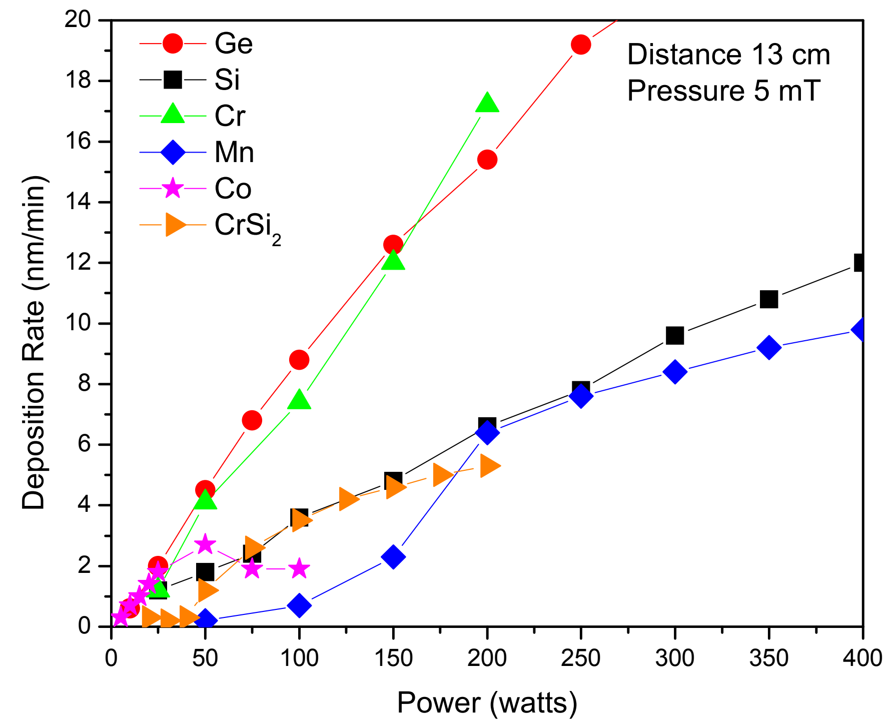

Y_2O_3 Stabilized ZrO_2 Substrate

Surface Roughness 500 nm

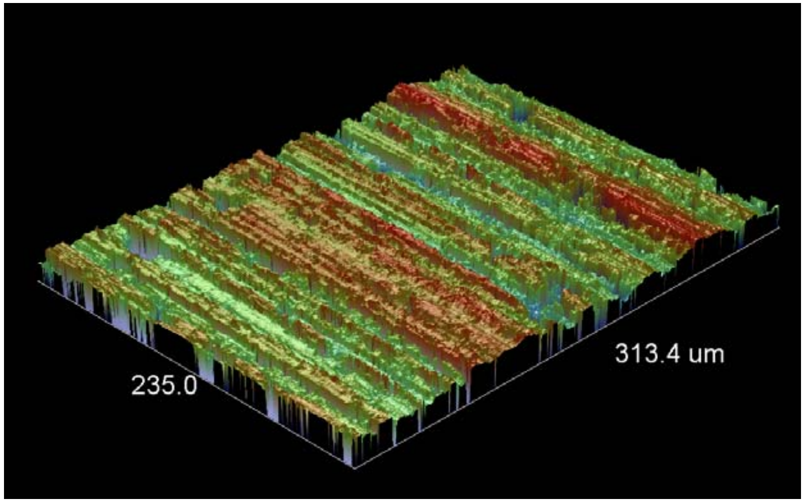

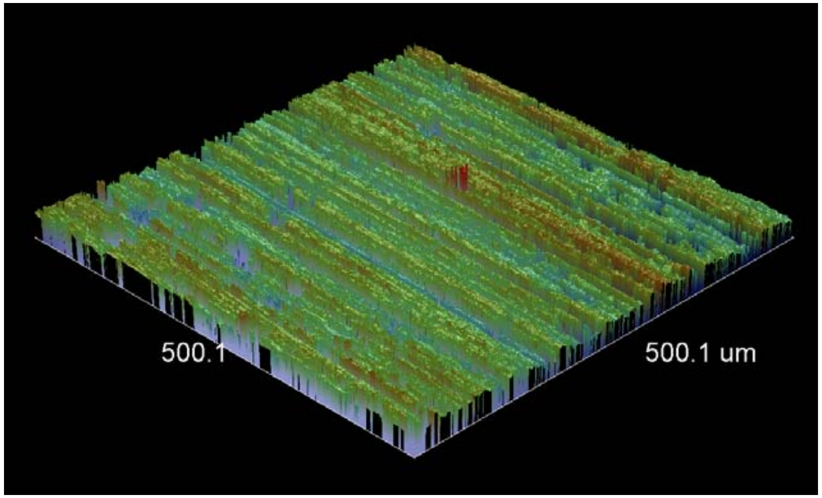

Deposit film retains the substrate surface roughness

YSZ ~ 2.5 W/mK Thermal Conductivity
11 x 10^{-6}/K Thermal Expansion

Total Film Stress = $\sigma_{TE} + \sigma_{process} + \sigma_{external}$

Film Failure is a Concern-Thickness > 1 μm

TE Property Measurements

Seebeck/Resistivity

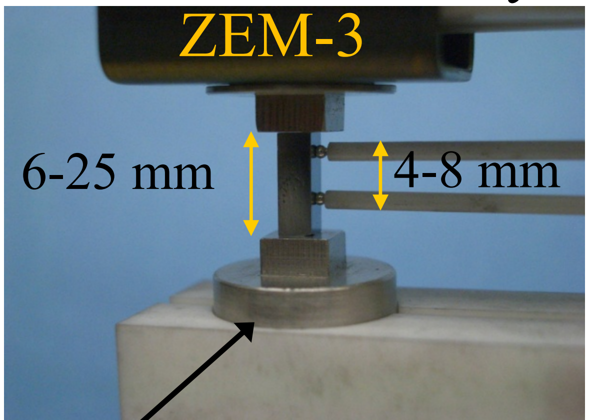

ΔT 0-50 °C/Furnace RT-1000 °C

Hall Measurement

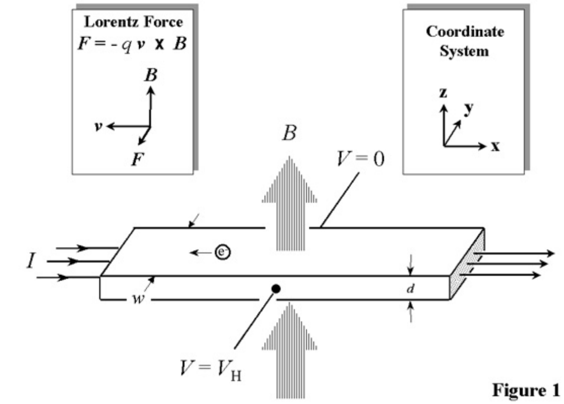

Capability-RT-527 °C/Field-2 Telsa

Silicide Film

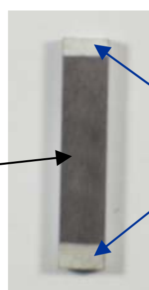

Ag Electrodes

Carrier Mobility & Density

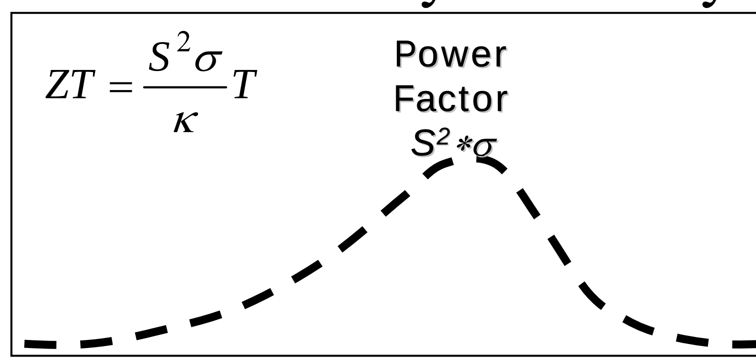

≈ 10^{19}
Carrier concentration [cm^{-3}]

Silicon Films

Si, B-Si, Sb-Si & Si/Ge Films

- Amorphous Films
- Deposition Temperatures – up to 750 °C
- High Resistivity – 10^9 Ω-m
- Anneal – 800 °C - Resistivity – 10^6 Ω-m

Metal Induced Crystallization

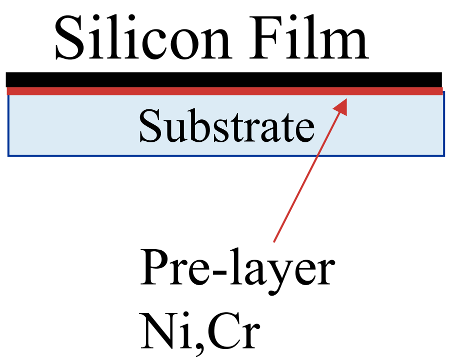

Lower Crystallization Temperature

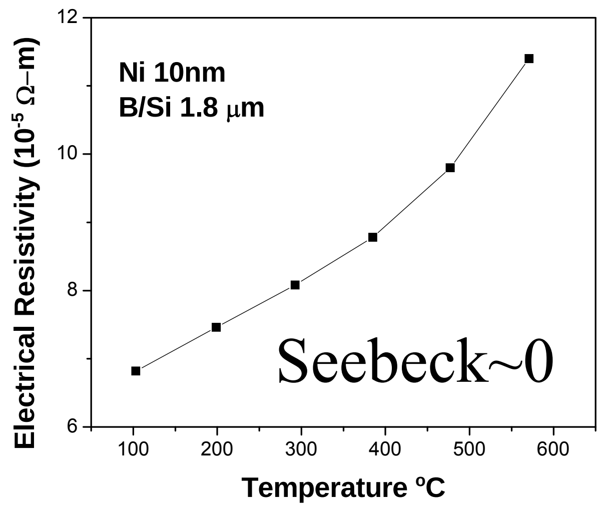

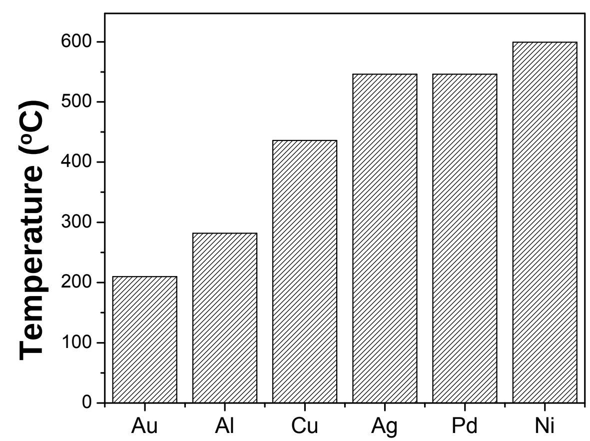

Knaepen et al., Thin Solid Films, 516, 4946, 2008

Mn-Si

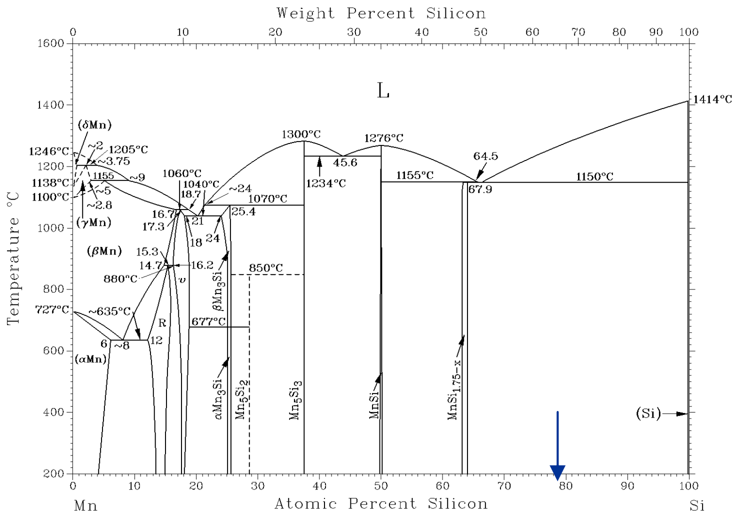

Deposition Temperature – 450 °C

XRD – Crystalline Phases – $Mn_{15}Si_{26}$

Film Thickness – 2.4 µm & 2.6 µm

800 °C Anneal

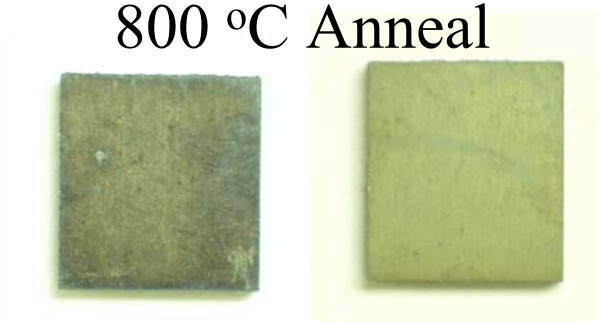

No Adhesion Failures – Tape Test

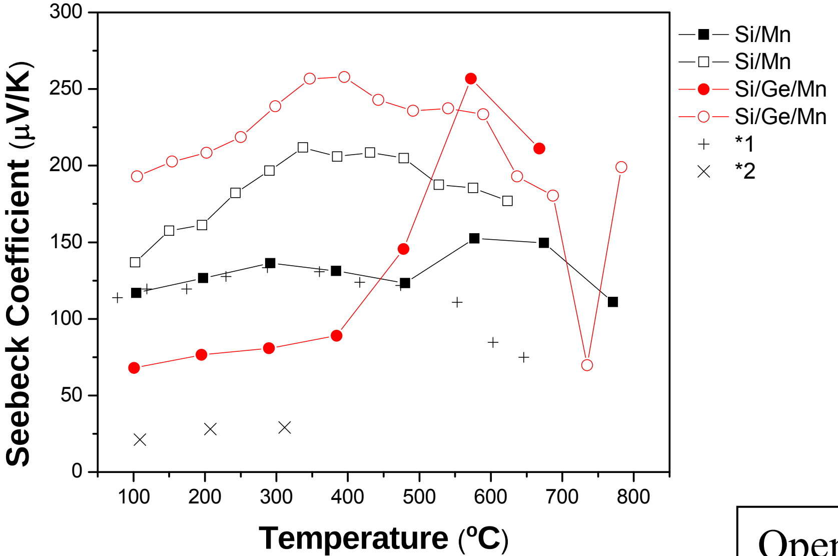

*1 Hou et al., Phy. Stat. Sol. A, 204, 3429, 2007

*2 Hou et al., Appl. Phys. A, 80, 1807, 2005

Open Symbols
2nd Measurement

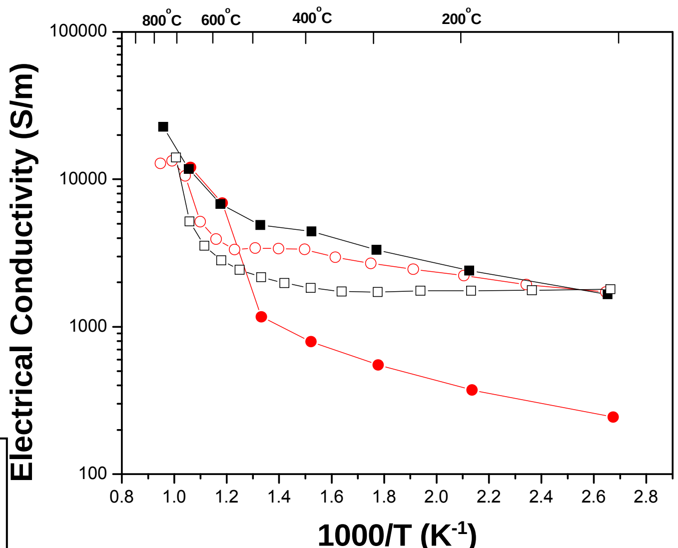

Mn-Si

Hall Measurements

Si/Mn 78/22 %	ρ (10^{-5} Ω–m)	Carrier ($1/cm^3$)	Mobility (cm^2/VS)
As Deposit	14.1	2×10^{21}	0.25
600°C-4 hrs	31	5×10^{20}	0.5
800°C-2 hrs	242	2×10^{20}	0.1

B-Si/Ge/Mn 61/37/2 %	ρ (10^{-5} Ω–m)	Carrier ($1/cm^3$)	Mobility (cm^2/VS)
As Deposit	280.1	6×10^{19}	0.3
600°C-4 hrs	40.8	6×10^{19}	2.6
800°C-2 hrs	50	2×10^{19}	7.3

Microstructure

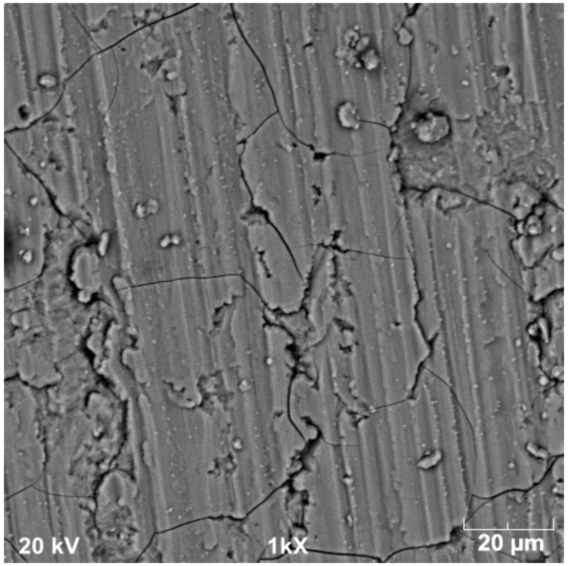

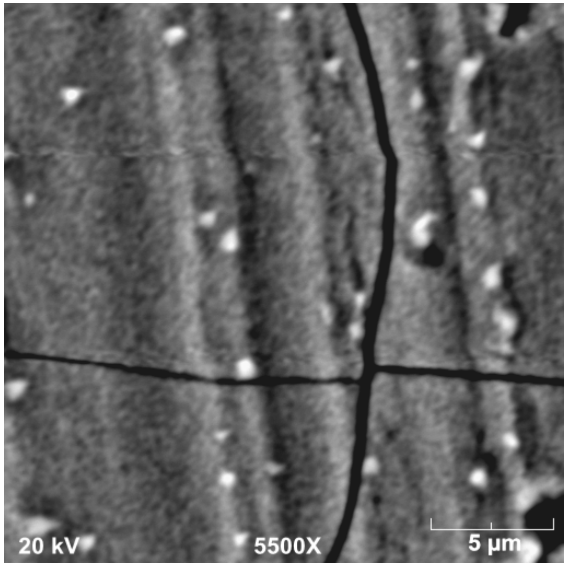

- Film Cracking
- No observable Grain Structure
- Defects due to Substrate

Co-Si

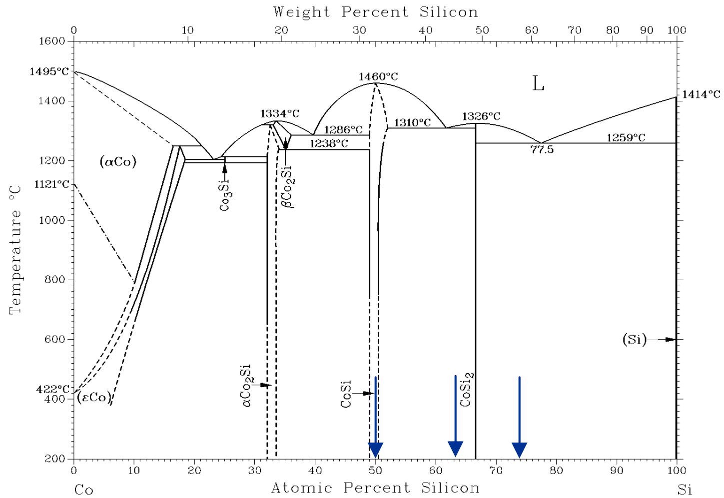

Deposition Temperature – 450 °C & 250 °C

Film Thickness – 1.5 µm & 1.8 µm

800 °C Anneal

No Adhesion Failures – Tape Test

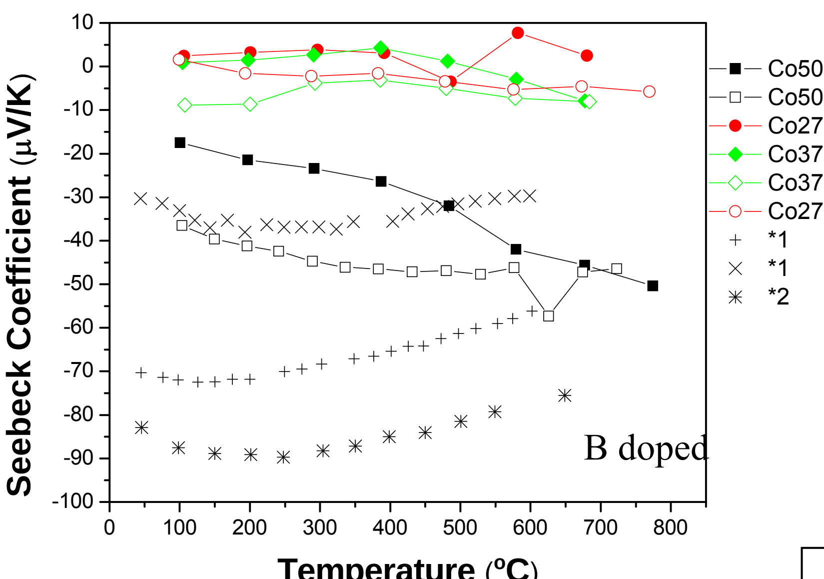

*1 Adachi et al., Mat. Sci. Forum, 426-432, 3445, 2003

*3 Ren et al., J. Alloys & Comp., 392, 50, 2005

Open Symbols
2nd Measurement

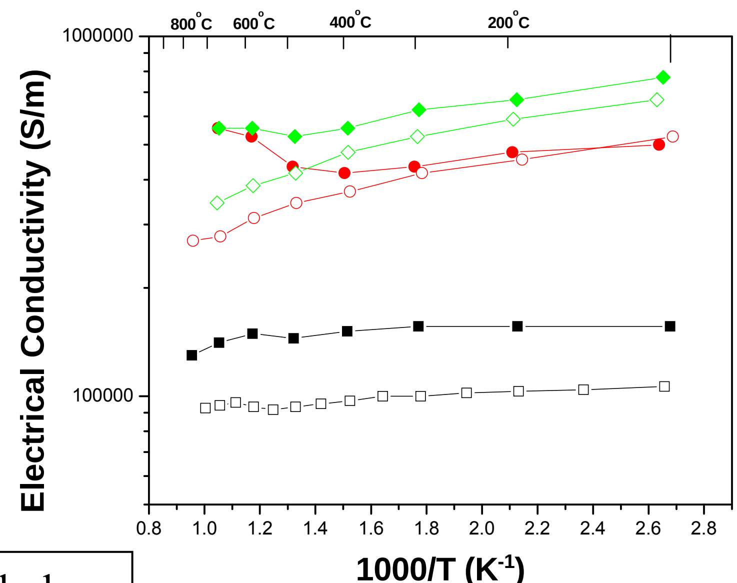

Co-Si

Hall Measurement

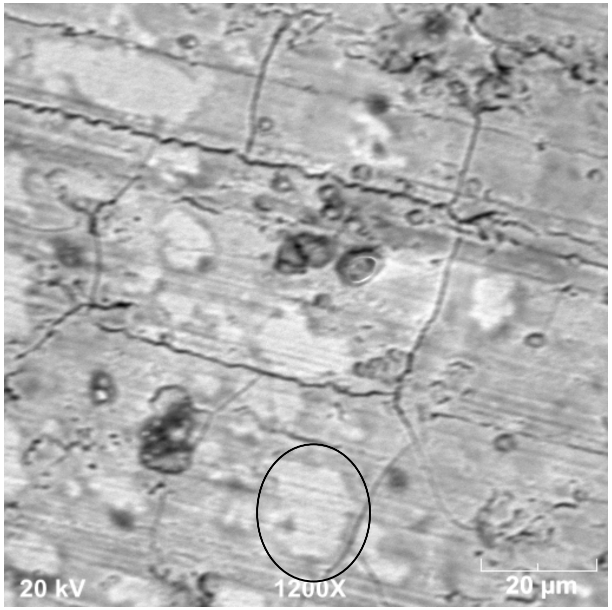

Si/Co 50/50 %	ρ (10^{-5} Ω–m)	Carrier ($1/cm^3$)	Mobility (cm^2/VS)
As Deposit	0.8	5×10^{20}	11
600°C-4 hrs	0.8	5×10^{20}	14
800°C-2 hrs	1.9	7×10^{20}	4

Sb-Si/Co 73/27 %	ρ (10^{-5} Ω–m)	Carrier ($1/cm^3$)	Mobility (cm^2/VS)
As Deposit	0.3	1×10^{22}	2.5
600°C-4 hrs	0.1	1.5×10^{22}	5
800°C-2 hrs	0.1	1×10^{22}	3

Sb-Si/Co 62/37 %	ρ (10^{-5} Ω–m)	Carrier ($1/cm^3$)	Mobility (cm^2/VS)
As Deposit	0.4	5×10^{21}	1.5
600°C-4 hrs	0.9	2×10^{22}	5
800°C-2 hrs	0.2	3×10^{22}	2

- Film Cracking
- No observable Grain Structure
- Defects due to Substrate
- Segregation?

Cr-Si

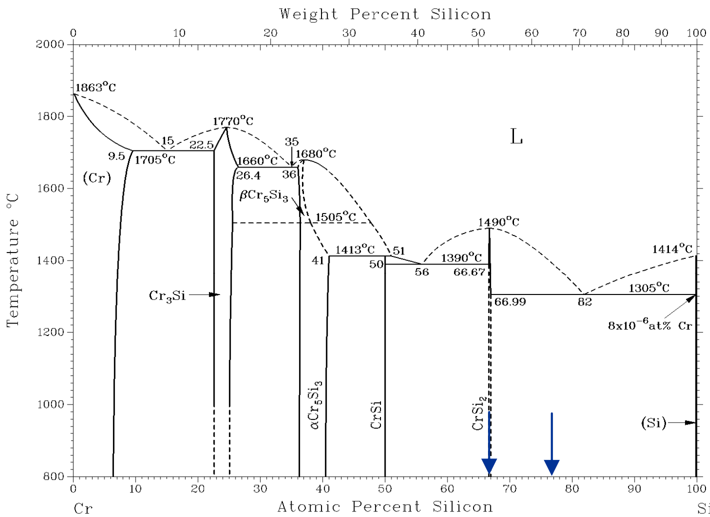

Deposition Temperature – 450 °C

XRD – Target $CrSi_2$- Poorly Crystallized

Co-sputtered – Crystalline $CrSi_2$

Film Thickness – 2.3 μm & 2.5 μm

800 °C Anneal

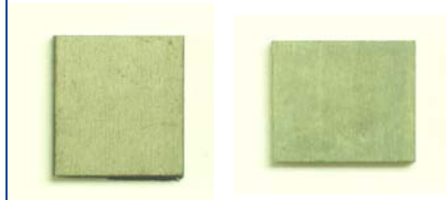

No Adhesion Failures – Tape Test

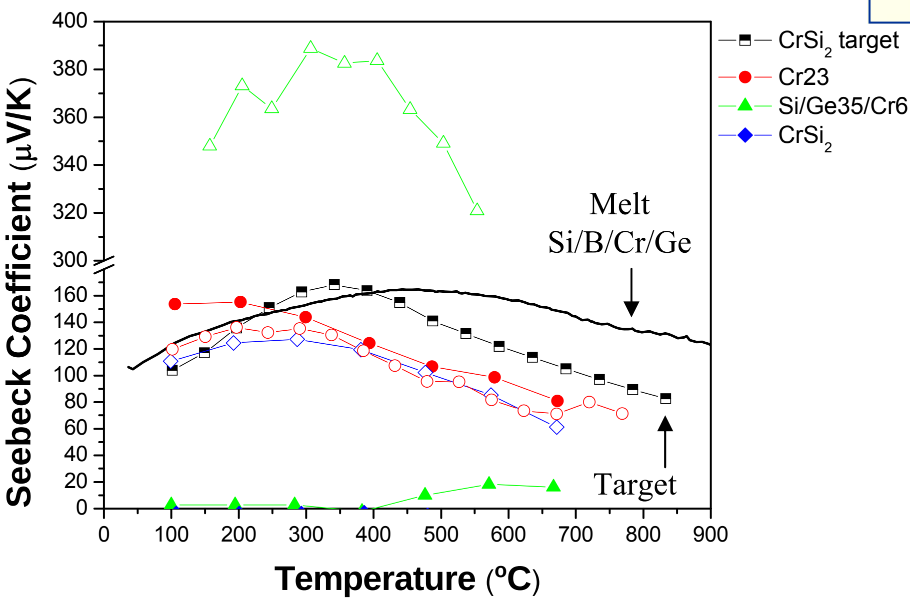

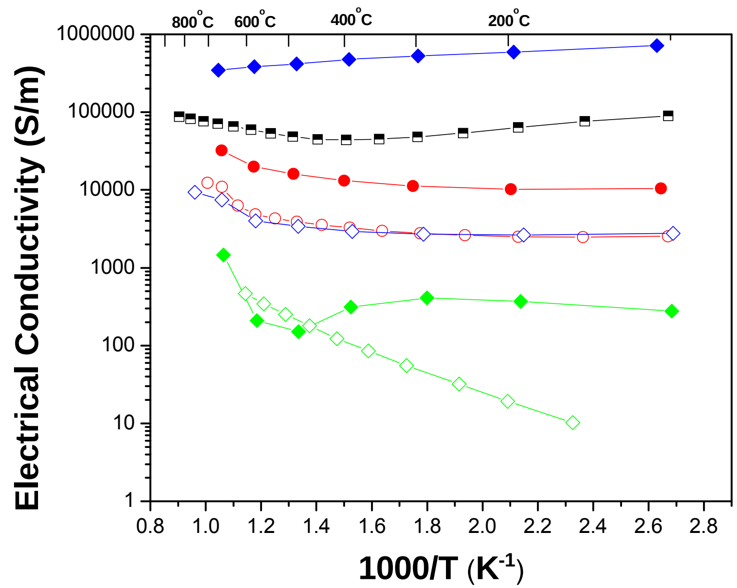

Cr-Si

$CrSi_2$ Target

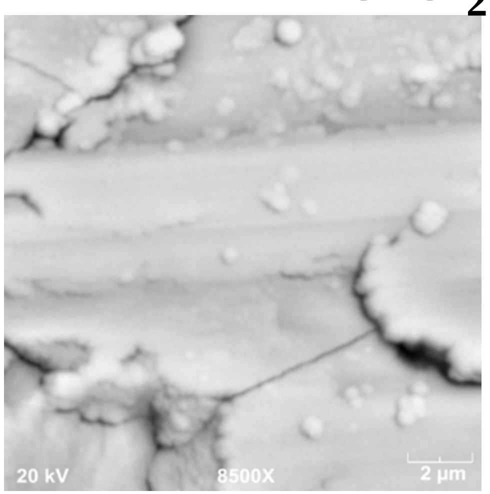

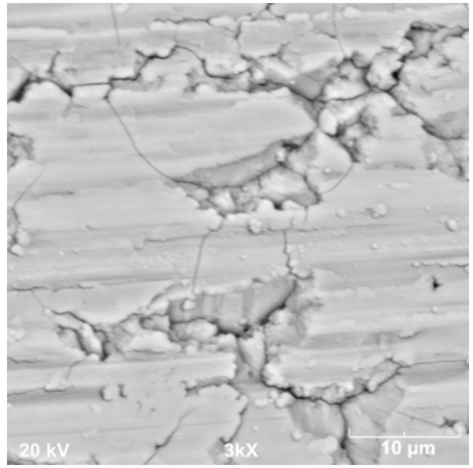

Hall Measurement

$CrSi_2$	ρ (10^{-5} Ω–m)	Carrier ($1/cm^3$)	Mobility (cm^2/VS)
As Deposit	9.2	1.5×10^{20}	1.4
600°C-4 hrs	37.3	1.7×10^{20}	1
800°C-2 hrs	775.4	6×10^{17}	10

- Film Cracking
- No observable Grain Structure
- Defects due to Substrate

Co-Sputtered

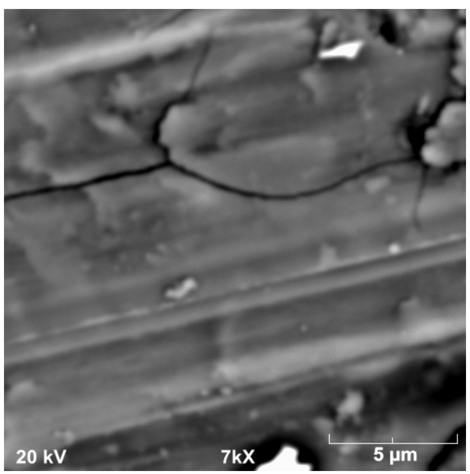

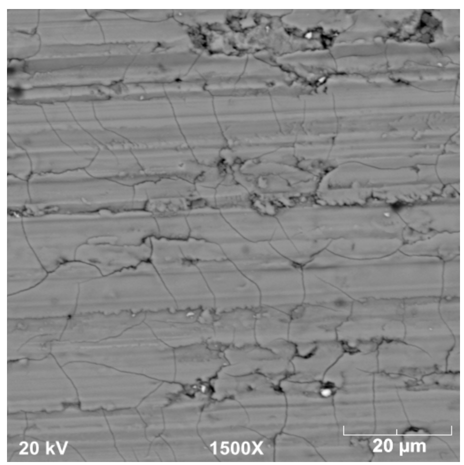

Hall Measurement

B-Si/Ge/Cr 59/35/6 %	ρ (10^{-5} Ω–m)	Carrier ($1/cm^3$)	Mobility (cm^2/VS)
As Deposit	428	1.5×10^{21}	0.1
600°C-4 hrs	269×10^5	2×10^{17}	1
800°C-2 hrs	219	3.2×10^{18}	8.8

Simple Module

Shadow Mask

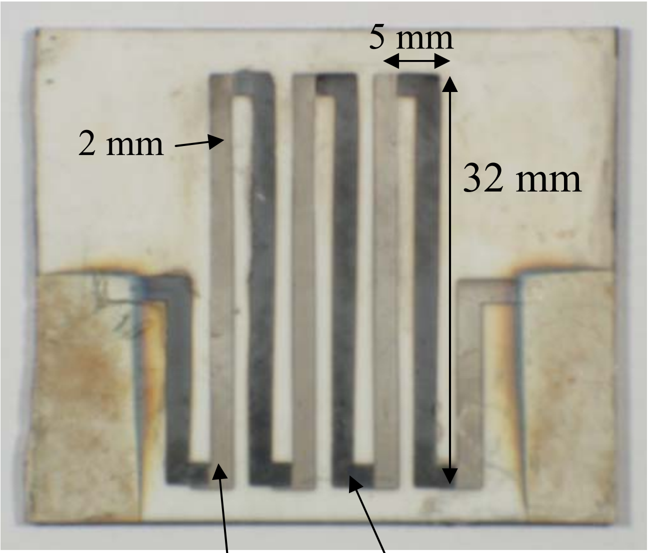

N-leg Pt   Si\Mn\Ge

Si\Mn\Ge
Large internal Ω
Legs ~ 40 MΩ
650 °C Anneal

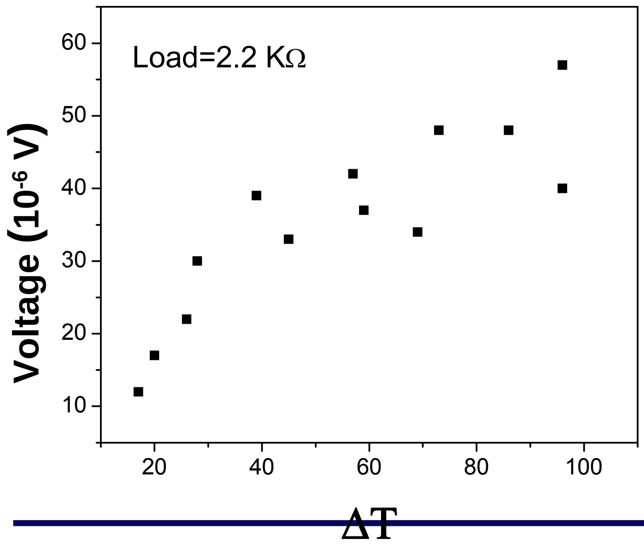

Power ≤ 10^{-12} watts

Summary

- Low resistive Si & Si/Ge difficult to achieve by magnetron sputtering.
- Low resistive films achieved with silicides of Co, Mn and Cr.
- Good Seebeck coefficients achieved for Mn & Cr silicides with P-type behavior.
- Moderate Seebeck coefficients achieved for Co silicides with N-type behavior.
- Silicide films exhibit low carrier mobility.
- Extensive film cracking is a problem.